Supporting Information

FeCo Nanoalloys Embedded in Nitrogen-Doped Carbon Nanosheets/Bamboo-like Carbon Nanotubes for Oxygen Reduction Reaction

Xiao-Wei Song,[1,2,4], Shuwei Zhang[1], Haihong Zhong[1], Yuan Gao[1], Luis A. Estudillo-Wong[5], Nicolas Alonso-Vante[3], Xin Shu[1,4,*] and Yongjun Feng[1,4,*]

1 State Key Laboratory of Chemical Resource Engineering, Beijing Engineering Center for Hierarchical Catalysts, College of Chemistry, Beijing University of Chemical Technology, No. 15 Beisanhuan East Road, Beijing 100029, China

2 Key Laboratory of Functional Coordination Compounds of Anhui Higher Education Institutes, School of Chemistry and Chemical Engineering, Anqing Normal University, Anqing 246011, China

3 IC2MP, UMR-CNRS 7285, University of Poitiers, F-86073 Poitiers Cedex 9, France

4 Anqing Research Institute, Beijing University of Chemical Technology, Anqing city, Anhui 24600, China

5 Departamento de Sociedad y Política Ambiental, CIIEMAD, Instituto Politécnico Nacional, Calle 30 de junio de 1520, C.P. 07340, CDMX, México

*Correspondence: shuxin@mail.buct.edu.cn (X. Shu), yjfeng@mail.buct.edu.cn (Y. J. Feng); Tel.: +86 10 6443 6992

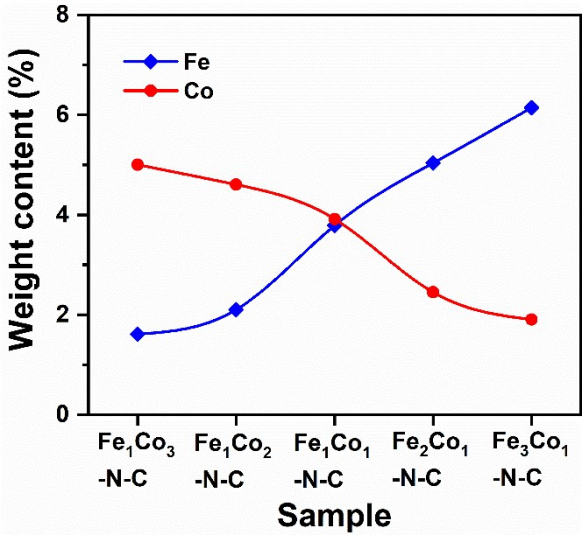

Figure S1. Weight content of Fe and Co obtained by ICP-AES

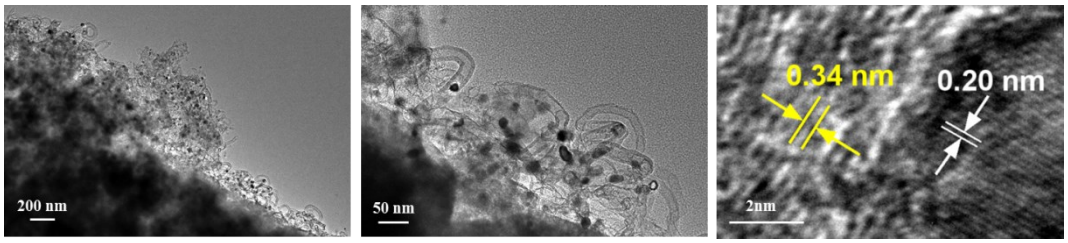

Figure S2. HRTEM images of the calcinated sample Fe_1Co_3-N-C

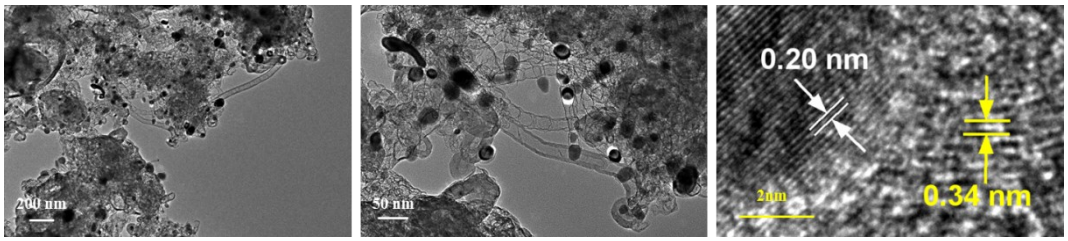

Figure S3. HRTEM images of the calcinated sample Fe_1Co_2-N-C

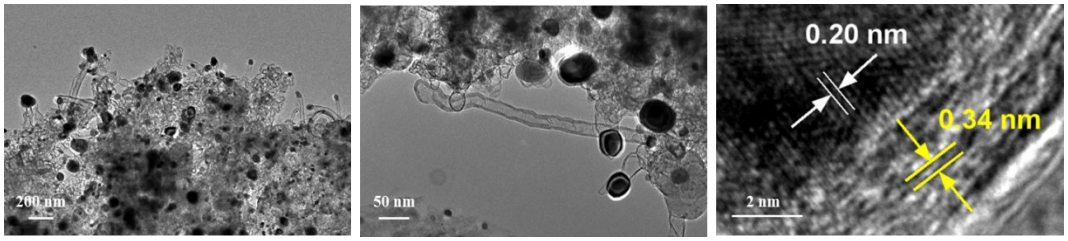

Figure S4. HRTEM images of the calcinated sample Fe_1Co_1-N-C

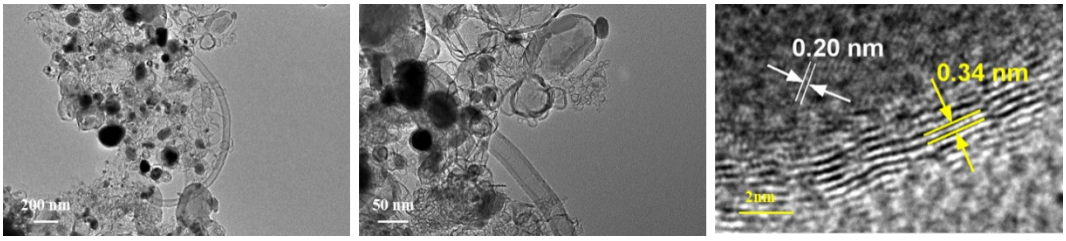

Figure S5. HRTEM images of the calcinated sample Fe_2Co_1-N-C

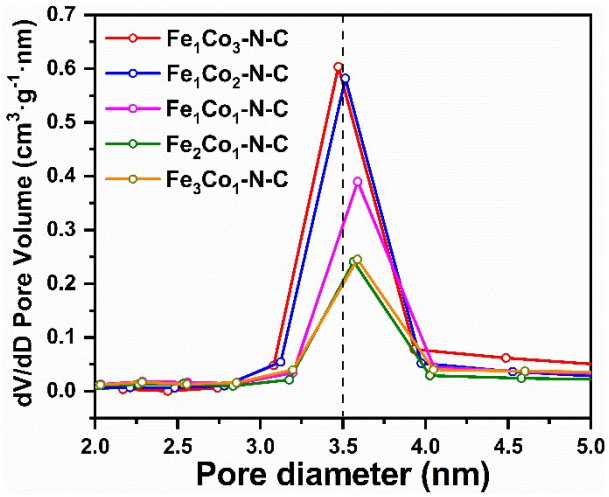

Figure S6. Pore diameter size distribution of the samples

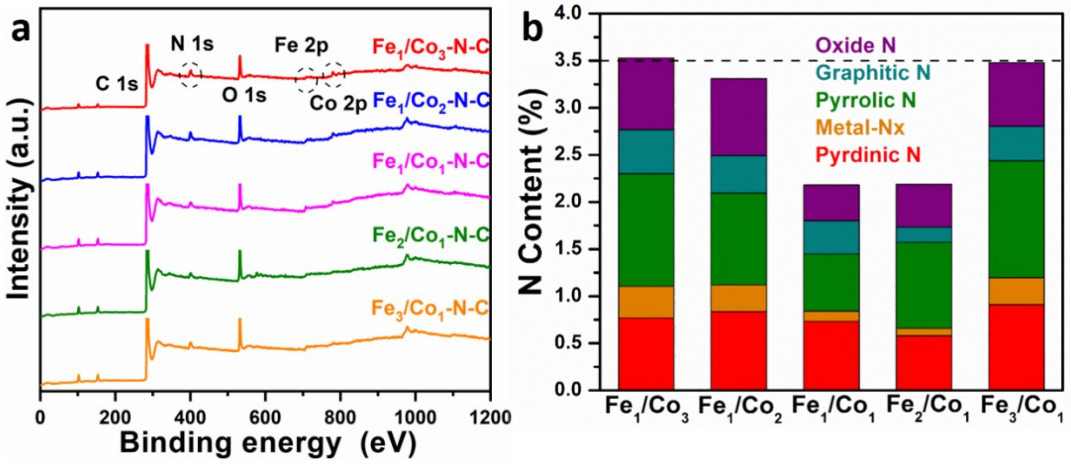

Figure S7. X-ray photoelectron spectra of all samples

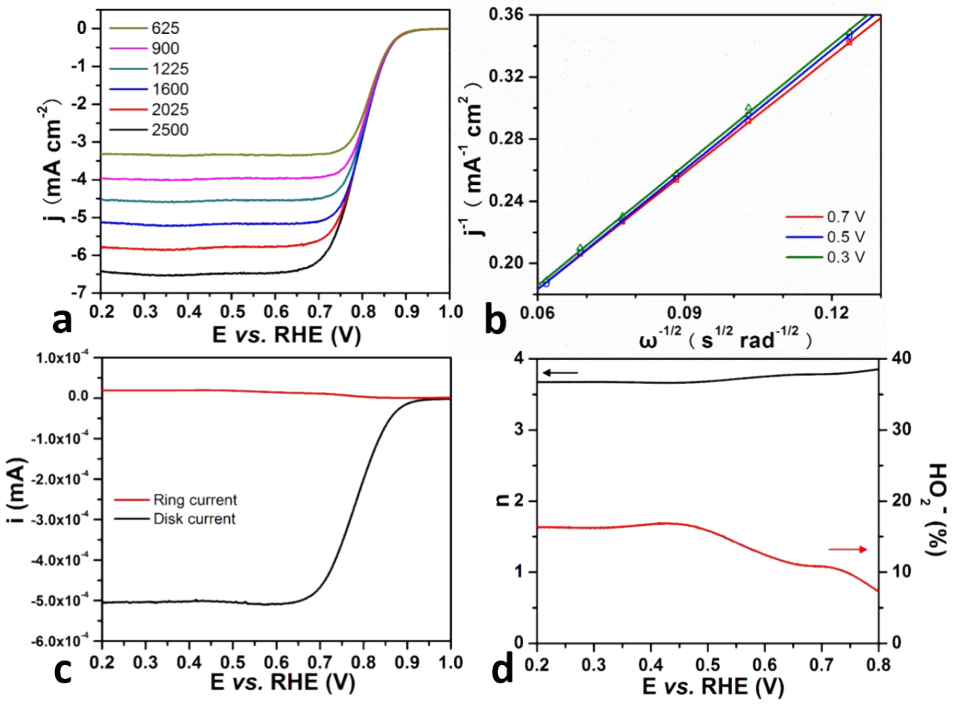

Figure S8. (a) Linear sweep voltammograms of Fe_1Co_3-N-C at rotating rates from 625 rpm to 2500 rpm in O_2-saturated 0.1M KOH. (b) K-L plots of Fe_1Co_3-N-C. (c) RRDE curve of Fe_1Co_3-N-C at 1600 rpm. (d) Peroxide yields and electron transfer numbers of Fe_1Co_3-N-C.

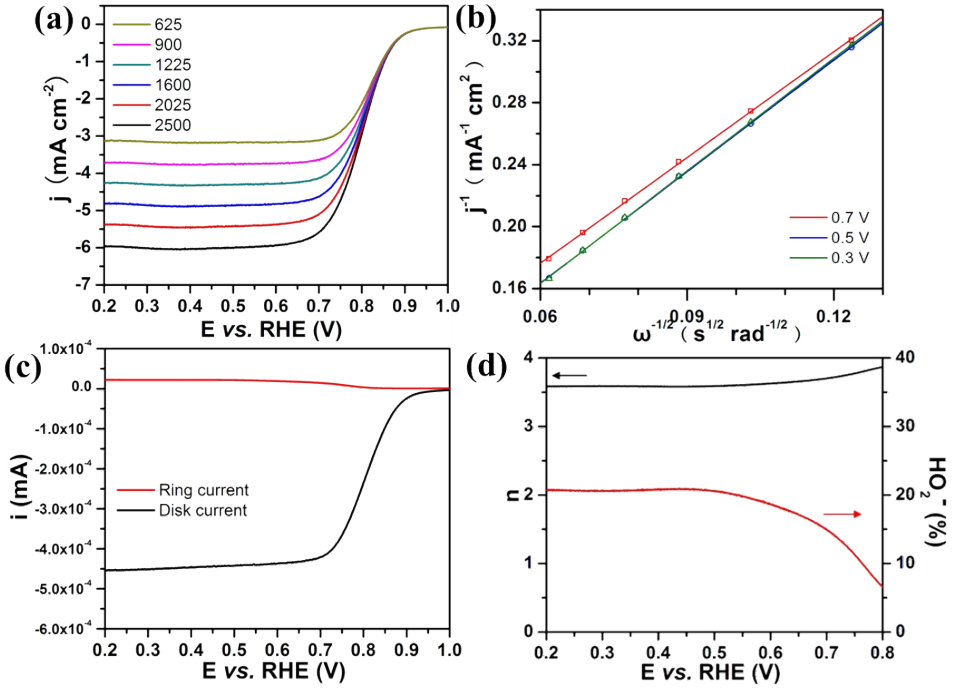

Figure S9. (a) Linear sweep voltammograms of Fe_1Co_2-N-C with rotating rates range from 625 rpm to 2500 rpm in O_2-saturated 0.1M KOH. (b) K-L plots of Fe_1/Co_2-N-C. (c) RRDE curve of Fe_1Co_2-N-C at 1600 rpm. (d) Peroxide yields and electron transfer numbers of Fe_1Co_2-N-C calculated by RRDE data.

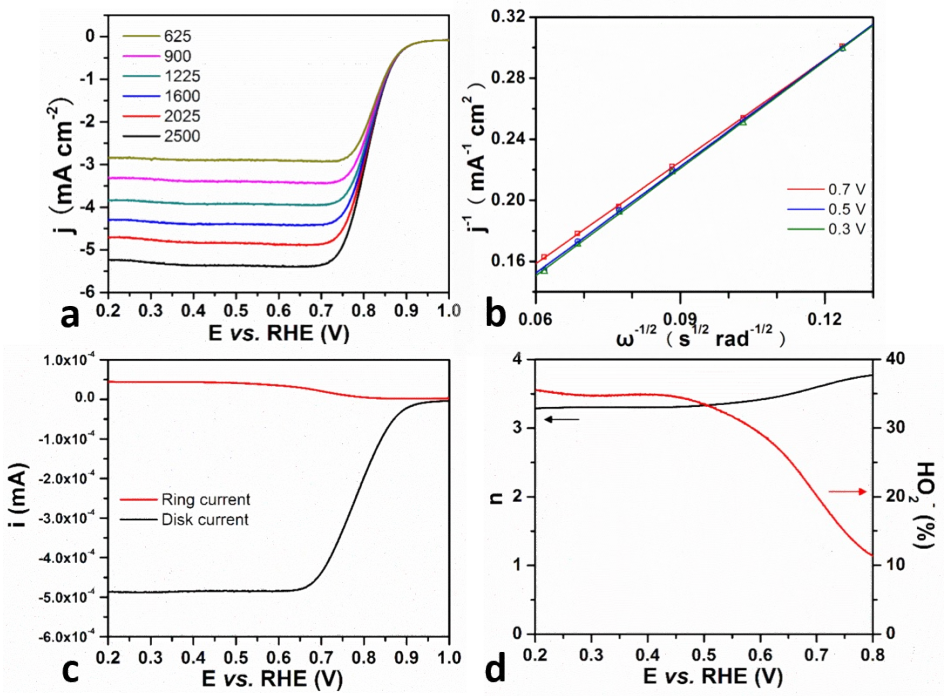

Figure S10. (a) Linear sweep voltammograms of Fe_1Co_1-N-C with rotating rates range from 625 rpm to 2500 rpm in O_2-saturated 0.1M KOH. (b) K-L plots of Fe_1/Co_1-N-C. (c) RRDE curve of Fe_1Co_1-N-C at 1600 rpm. (d) Peroxide yields and electron transfer numbers of Fe_1Co_1-N-C.

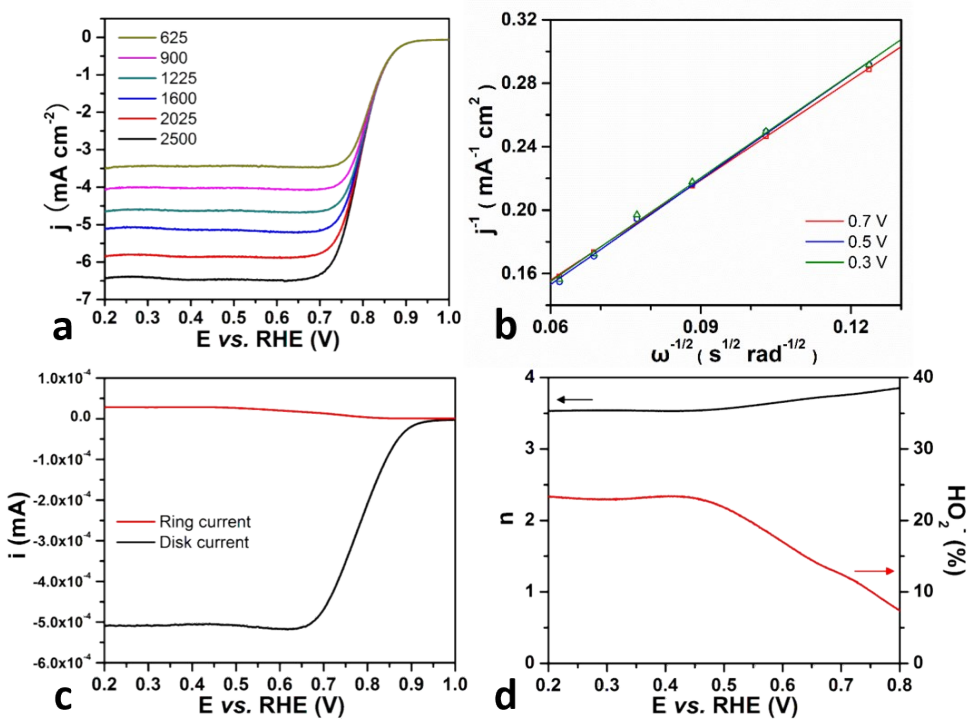

Figure S11. (a) Linear sweep voltammograms of Fe_2/Co_1-N-C with rotating rates range from 625 rpm to 2500 rpm in O_2-saturated 0.1M KOH. (b) K-L plots of Fe_2/Co_1-N-C. (c) RRDE curve of Fe_2Co_1-N-C at 1600 rpm. (d) Peroxide yields and electron transfer numbers of Fe_2Co_1-N-C.

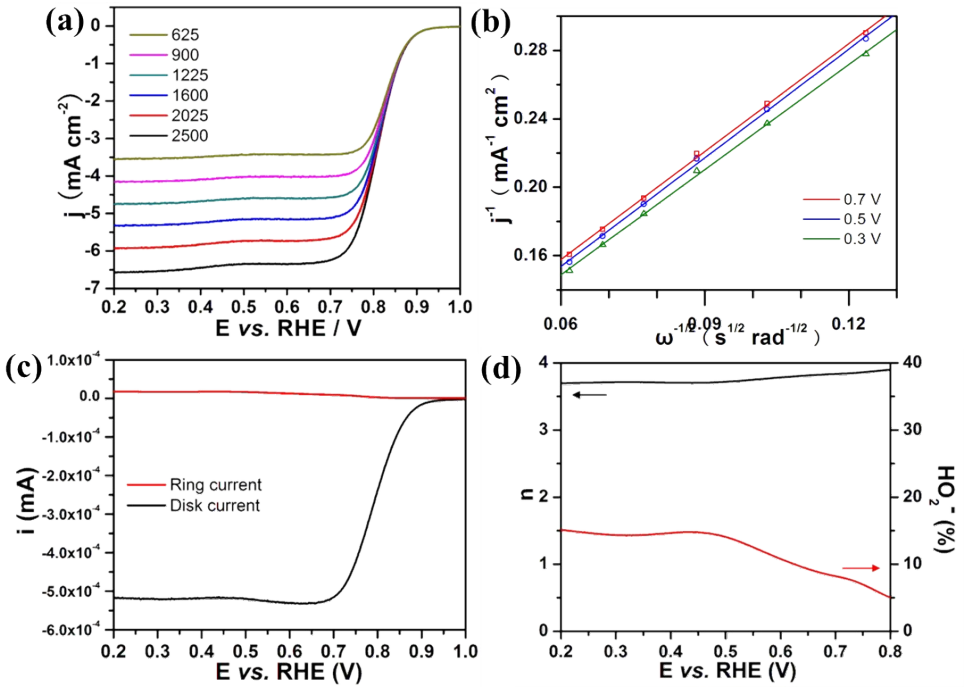

Figure S12. (a) Linear sweep voltammograms of Fe_3/Co_1-N-C with rotating rates range from 625 rpm to 2500 rpm in O_2-saturated 0.1M KOH. (b) K-L plots of Fe_3/Co_1-N-C. (c) RRDE curve of Fe_3Co_1-N-C at 1600 rpm. (d) Peroxide yields and electron transfer numbers of Fe_3Co_1-N-C.

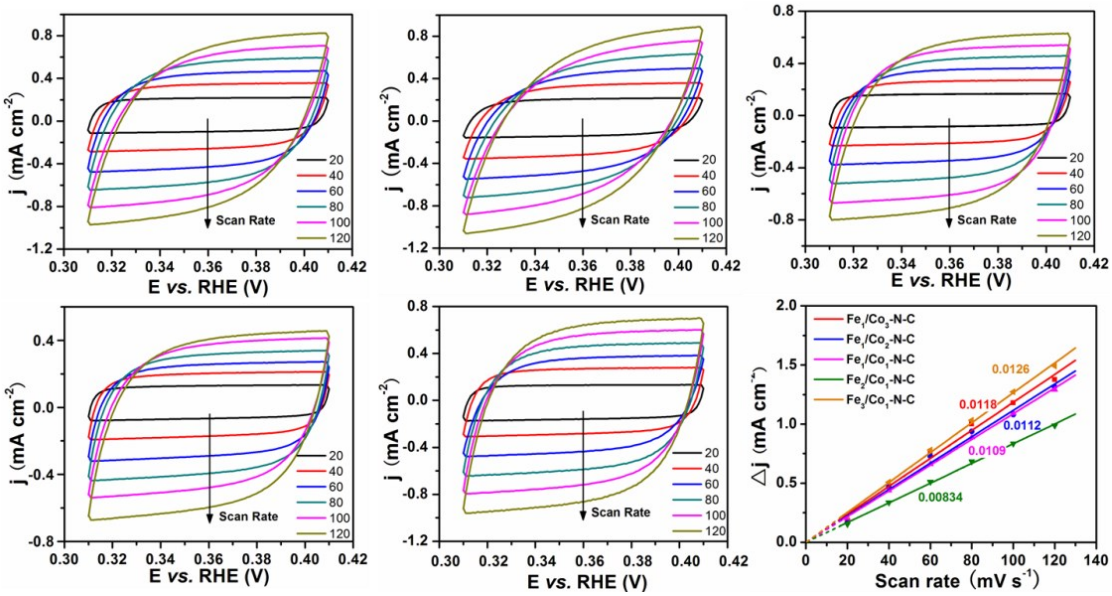

Figure S13. (a-e) CV curves for the electrochemical double-layer capacitance at different scan rates in N_2-saturated KOH solution; (f) C_{dl} calculation of all samples.

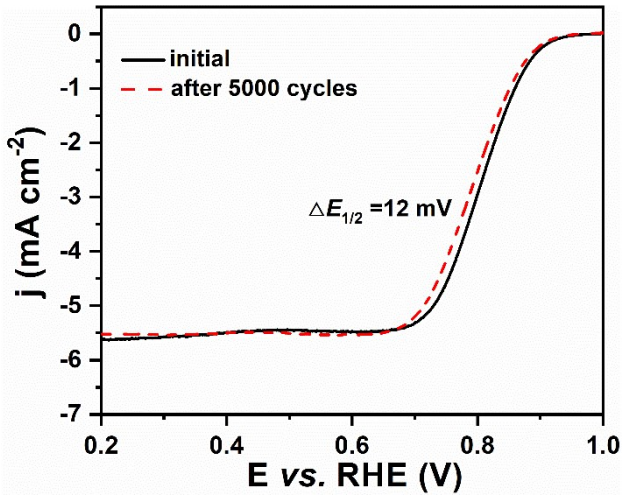

Figure S14. The ORR-LSV curves of Fe_3Co_1-N-C catalyst at 1600 rpm before/after the accelerated stability tests with 100 mV s^{-1} in O_2-saturated 0.1 M KOH solution.

Table S1. The ORR parameters of Fe_3Co_1-N-C and other bimetallic FeCo-based multicomponent supported on N-doped carbon materials reported in the literatures.

Catalyst	$E_{1/2}$ (V)	j_L (mA cm^{-2})	Tafel slope (mV dec^{-1})	n	Mass load (mg cm^{-2})	Ref.
Fe_1Co_3-N-C	0.81	5.18	65.6	3.7	0.228	This work
Fe_3Co_1-N-C	0.82	5.25	59.9	3.7	0.228	This work
FeCo@N-GCNT-FD	0.88	6.8	-	3.96	0.479	[1]
$Fe_{0.3}Co_{0.7}$/NC cages	0.88	6.1	79	3.87	0.25	[2]
meso/micro-FeCo-Nx-CN-30	0.886	6.3	-	-	0.1	[3]
CoFe/N-GCT	0.79	4.86	74	-	0.597	[4]
N-C-CoFe	0.7	5.0	59	3.9	-	[5]
$Co_{1.08}Fe_{3.34}$@NGT	0.94	7.4	44	~4	0.202	[6]
FeCo@MNC	0.86	5.2	66	3.87	0.36	[7]
FeCo-ISAs/CN	0.92	6.1	57	3.9-4.0	0.408	[8]
Fe-Co-N-C	0.76	7.5	-	-	0.635	[9]
Fc-F/Co@N-C800	0.86	4.9	65.1	3.83	0.2	[10]
(Fe,Co)/CNT	0.95	4.9	-	3.95	0.501	[11]
CoFe/NC-0.2-900	0.82	6.4	73	3.91	0.1	[12]
FeCo@NCs-0.15	0.83	5.75	73	3.85	-	[13]

All the data was obtained from the RDE measurements with a rotating speed of 1600 rm in O_2-saturated 0.1 M KOH solution.

References

1. L. An, N. Jiang, B. Li, S. Hua, Y. Fu, J. Liu, W. Hao, D. Xia and Z. Sun, A highly active and durable iron/cobalt alloy catalyst encapsulated in N-doped graphitic carbon nanotubes for oxygen reduction reaction by a nanofibrous dicyandiamide template, *J. Mater. Chem. A*, 2018, **6**, 5962-5970.
2. B. Y. Guan, Y. Lu, Y. Wang, M. Wu and X. W. Lou, Porous Iron–Cobalt Alloy/Nitrogen-Doped Carbon Cages Synthesized via Pyrolysis of Complex Metal–Organic Framework Hybrids for Oxygen Reduction, *Adv. Funct. Mater.*, 2018, **28**, 1706738.
3. S. Li, C. Cheng, X. Zhao, J. Schmidt and A. Thomas, Active Salt/Silica-Templated 2D Mesoporous FeCo-Nx-Carbon as Bifunctional Oxygen Electrodes for Zinc–Air Batteries, *Angew. Chem. Int. Ed.*, 2018, **57**, 1856-1862.
4. X. Liu, L. Wang, P. Yu, C. Tian, F. Sun, J. Ma, W. Li and H. Fu, A Stable Bifunctional

Catalyst for Rechargeable Zinc–Air Batteries: Iron–Cobalt Nanoparticles Embedded in a Nitrogen-Doped 3D Carbon Matrix, *Angew. Chem. Int. Ed.*, 2018, **57**, 16166-16170.

5. A. Samanta and C. R. Raj, Catalyst Support in Oxygen Electrocatalysis: A Case Study with CoFe Alloy Electrocatalyst, *J. Phys. Chem. C*, 2018, **122**, 15843-15852.

6. S. Sultan, J. N. Tiwari, J.-H. Jang, A. M. Harzandi, F. Salehnia, S. J. Yoo and K. S. Kim, Highly Efficient Oxygen Reduction Reaction Activity of Graphitic Tube Encapsulating Nitrided CoxFey Alloy, *Adv. Energy Mater.*, 2018, **8**, 1801002.

7. C. Li, M. Wu and R. Liu, High-performance bifunctional oxygen electrocatalysts for zinc-air batteries over mesoporous Fe/Co-N-C nanofibers with embedding FeCo alloy nanoparticles, *Appl. Catal. B: Environ.*, 2019, **244**, 150-158.

8. D. Zhang, W. Chen, Z. Li, Y. Chen, L. Zheng, Y. Gong, Q. Li, R. Shen, Y. Han, W.-C. Cheong, L. Gu and Y. Li, Isolated Fe and Co dual active sites on nitrogen-doped carbon for a highly efficient oxygen reduction reaction, *Chem. Commun.*, 2018, **54**, 4274-4277.

9. L. Osmieri, C. Zafferoni, L. Wang, A. H. A. Monteverde Videla, A. Lavacchi and S. Specchia, Polypyrrole-Derived Fe−Co−N−C Catalyst for the Oxygen Reduction Reaction: Performance in Alkaline Hydrogen and Ethanol Fuel Cells, *ChemElectroChem*, 2018, **5**, 1954-1965.

10. M. Tan, T. He, J. Liu, H. Wu, Q. Li, J. Zheng, Y. Wang, Z. Sun, S. Wang and Y. Zhang, Supramolecular bimetallogels: a nanofiber network for bimetal/nitrogen co-doped carbon electrocatalysts, *J. Mater. Chem. A*, 2018, **6**, 8227-8232.

11. J. Wang, W. Liu, G. Luo, Z. Li, C. Zhao, H. Zhang, M. Zhu, Q. Xu, X. Wang, C. Zhao, Y. Qu, Z. Yang, T. Yao, Y. Li, Y. Lin, Y. Wu and Y. Li, Synergistic effect of well-defined dual sites boosting the oxygen reduction reaction, *Energy Environ. Sci.*, 2018, **11**, 3375-3379.

12. Z. Du, P. Yu, L. Wang, C. Tian, X. Liu, G. Zhang and H. Fu, Cubic Imidazolate Frameworks-Derived CoFe Alloy Nanoparticles-Embedded N-doped Graphitic Carbon for Discharging Reaction of Zn-air Battery, *Sci. China Mater.* 2020, **63**, 327-338.

13. X. Luo, H. Ren, H. Ma, C. Yin, Y. Wang, X. Li, Z. Shen, Y. Wang and L. Cui, In situ integration of Co5.47N and Co0.72Fe0.28 alloy nanoparticles into intertwined carbon network for efficient oxygen reduction, *J. Colloid Interf. Sci.*, 2020, **569**, 267-276.